Institute of Space and Aeronautical Science, University of Tokyo
Report No. 443, February 1970

The Characteristics of the Hot Torsion Test for Assessing Hot Workability of Aluminum Alloys

By

Ryo HORIUCHI, Junichi KANEKO, A. B. ELSEBAI
and M. M. SULTAN

Summary: Experimental discussions were given in some detail on the characteristics of the hot torsion test, and an adequate way to evaluate hot workability of aluminum alloys under hot working conditions was discussed. The most important point is that heat generated by the work of deformation causes temperature rise, nonuniform temperature distributions and hence nonuniform distributions in shear strain in the specimen. Taking the effects of temperature rise into consideration, the solid cylindrical specimen test is preferred to the tubular specimen and differential test, and shorter guage length is desirable. Temperature change in the specimen was measured during torsional deformation, and a reasonable agreement was obtained between the measured values and the calculated ones which were obtained by solving the differential equations of nonsteady heat transfer with proper boundary conditions.

1. INTRODUCTION

Accompanying with recent rapid growth of aluminum production, large scaled processing equipments for rolling or extrusion, which are operated at high speed, have become of wide use. In order to operate such equipments efficiently, the hot workability of the material to be processed must be evaluated at the same working temperature and strain rate by means of some laboratory tests.

Hot workability, here, is defined to be the combination of deformation resistance and ductility of the material, with more emphasis on the latter. Hot workability itself is not expressed quantitatively, and discussion will be carried out separately for flow stress and ductility. Hot workability is not solely a property of the material concerned, but differs from one hot working process to the other. Therefore, it should be evaluated by the test simulating a particular hot working process property. However, the hot workability test is usually done by deforming the material under the conditions where the analysis of the stress-strain relation is easily carried out. The results of such tests cannot therefore be applied directly to each actual hot working process. Even those simpler deformation encountered in the hot workability test, the test results obtained are affected by the various testing conditions. Therefore, it should be noted that all the results of the hot workability test show the quantity depending both on the material and on the various testing conditions.

In this paper, a detailed discussion is presented on the characteristics of the hot torsion testing method in order to study the effect of testing conditions on the test results and furthermore to determine the optimum testing conditions. This kind of study is important as the first step before investigating hot workability of various aluminum alloys by means of the hot torsion test.

Recently, the hot torsion test is of frequent use for assessing hot workability of metals, particularly for steels. The advantages and disadvantages of the hot torsion test in comparison with the other testing methods have been discussed elsewhere [1, 2, 3]. The most important advantage of the hot torsion test is its capability to carry out the deformation in such a way that it can simulate the industrial hot working processes better than any other laboratory testing methods such as the hot tension or compression test. However, since deformation is done at high strain rate up to very high strain in the hot torsion test, the work done for deformation will cause considerable rise in temperature of the specimen during deformation. Since heat is conducted away to the grip section of the specimen, temperature distribution with a maximum at the middle will therefore result. Tsubouchi and Kudo [4] measured temperature change during torsional deformation of the tubular specimens of mild steel deformed at room temperature. They also obtained an equation to estimate the amount of temperature rise by solving a differential equation of heat conduction. In this work, temperature rise was measured for the solid cylindrical specimens of aluminum alloys twisted at 400°C and an equation was derived to estimate the amount of temperature rise. A reasonable agreement was obtained between the measured and calculated values. Furthermore, a detailed discussion is given for the effect of temperature rise on the results of the hot torsion test. It is also shown that distribution of temperature rise is varied with the testing conditions and the shape and dimensions of the specimens used. Therefore, the uniformity of torsional strain is significantly affected by those, and hence the values of strain to fracture.

It is therefore important to study how strain to fracture changes with the testing conditions and the shape and dimensions of the specimen. Without this study, study of ductility by means of the hot torsion test is rather meaningless, but this kind of problems seem to remain to be clarified. In this work, the effects of the testing conditions and the shape and dimensions of the specimen on the values of fracture strain in the hot torsion test of aluminum alloys have been discussed. And, it is shown to be closely related to the temperature rise during deformation. Further, the optimum testing conditions and specimen dimensions have been determined for the hot torsion test of aluminum alloys.

2. Experimental Procedure

A torsion testing machine was designed and constructed. This machine can subject the specimen to torsional deformation at a constant twisting rate in the range of 10 to 2,500 rpm. The specimen is held at high temperature in the electrical resistance furnace attached to the testing machine, and testing is carried out in the air.

During deformation, one end of the specimen is kept free to the axial strain which is measured throughout torsional deformation. In some cases, the axial tensile load is applied to this free end to carry out torsional deformation under the combined stress. A sketch of the torsion testing machine used in this work is shown in Fig. 1.

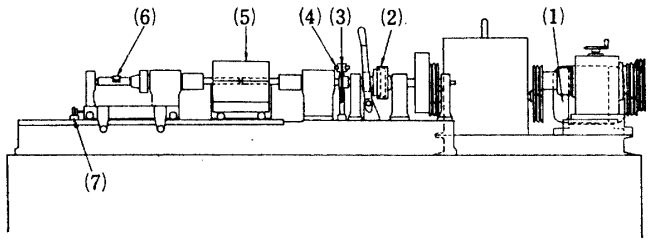

FIG. 1. The torsion testing machine
1: motor, 2: clutch, 3: perforated round plate, 4: photo cell, 5: electrical resistance furnace, 6: load cell, 7: strain guage

TABLE 1. Chemical composition of the alloys used

Alloy	Fe	Si	Cu	Mg	Mn	Cr
3003 (3S)	0.51	0.11	0.03	—	1.2	—
5052 (52S)	0.21	0.10	0.04	2.1	—	0.25
5056 (56S)	0.16	0.08	0.01	4.6	0.06	0.08
2017 (17S)	0.24	0.30	3.9	0.58	0.49	—

The values of torque, angle of twist and axial strain are recorded by the oscillograph, and the values of torque and angle of twist are converted to shear stress and shear strain respectively. Torsional deformation is carried out in the ranges of temperature 300 to 500°C and of strain rate at the surface of the specimen 1 to 100 sec^{-1}. The specimen used are machined out of the extruded rods of aluminum alloys, 3003, 5052, 2017 and 5056. Chemical compositions of the alloys used are listed in Table 1. A sketch of the specimen is shown in Fig. 2.

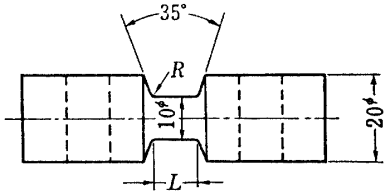

FIG. 2. Sketch of the specimen

Temperature change was measured during torsional deformation at the middle of the deformed section of the specimen either at the center or at the outernal surface for some specimens particularly designed and machined for this purpose. For measuring temperature at the middle-center of the specimen, a thin hole of 2 mm diameter was drilled through along the center axis from one end to the middle where a chromel-alumel thermocouple was inserted. For the middle-surface, the hot junction of 0.1 mm thermocouple wire was inserted at the depth of 1.5 mm from the surface. Recording of temperature was done by the 10 mV full scale recorder of which the response time for the full scale was 1 sec.

3. Torsional Deformation of the Cylindrical Specimens

In torsional deformation, the values of torque and angle of twist are usually measured, and it is necessary to convert these values into shear stress and shear strain respectively. For conversion of torque into shear stress at the surface of the solid cylindrical specimens, one of the following three equations may be applied:

$$\tau_a=\frac{3M}{2\pi a^3} \tag{1}$$

$$\tau_a=\frac{M}{2\pi a^3}\left(3+\frac{\partial lnM}{\partial ln\theta}\right) \tag{2}$$

$$\tau_a=\frac{M}{2\pi a^3}\left(3+\frac{\partial lnM}{\partial ln\theta}+\frac{\partial lnM}{\partial ln\dot{\theta}}\right) \tag{3}$$

where, τ_a: shear stress at the surface
M: torque of torsional deformation
a: radius of the specimen
θ: angle of twist, and $\dot{\theta}$ is angular velocity of twist.

Equation (1) is applicable to ideally plastic materials, and Equation (2) is valid for materials of which the stress-strain relation is generally expressed as $\tau=f(\gamma)$ and called Nadai's equation. Equation (3), on the other hand, is used for materials of which flow stress is a function of both strain and strain rate [5]. Since metals show strain rate dependency of flow stress at high temperature, Equation (3) is considered to be most suitable for the hot torsion test among above three equations.

However, the decrease in flow stress at higher strain usually occurs in the hot torsion test, because of temperature rise in the specimen. When the isothermal stress-strain relation is of direct interest, the obtained values of torque need to be corrected with respect to temperature rise. In such a case, the following equation may be used,

$$\tau'_a=\frac{1}{2\pi a^3}\left[M-\left(\frac{\partial M}{\partial T}\right)\Delta T\right]\left(3+\frac{\partial lnM}{\partial ln\theta}+\frac{\partial lnM}{\partial ln\dot{\theta}}\right) \tag{4}$$

where, τ'_a is corrected shear stress with respect to temperature rise, ΔT. The observed values of temperature rise in the specimen during the hot torsion test of aluminum alloys are presented below along with the method of its numerical estimation.

Fig. 3 shows shear stress-shear strain curves obtained by using Equation (4) for the specimens of the alloy 5052 tested at 400°C at different strain rates, and for comparison, curves obtained by using Equation (3) are also shown in the dotted lines for the same testing conditions. It is seen that deviation of the uncorrected curves increases as increasing strain, and that the corrected curves remain to show the strain rate dependency even at higher strain. Therefore, in comparing the flow stress values of different strain rates and testing temperatures from the uncorrected

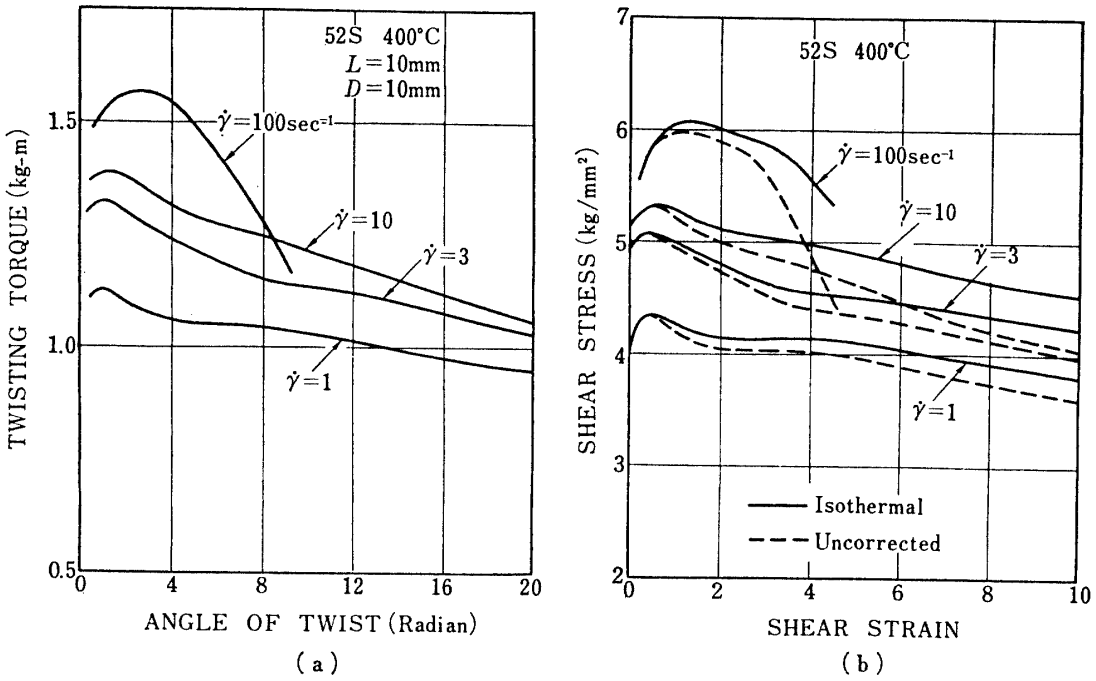

FIG. 3. Conversion of record torque-twist curves (a) into shear stress-shear strain curves (b) for different strain rate. The isothermal curves are compared with uncorrected ones.

shear stress values, shear stress at lower strain must be taken where deviation due to temperature rise is negligibly small.

The term for the strain rate correction can be evaluated from the logarithmic plot of M vs. $\dot{\theta}$, such as shown in Fig. 4, where $\dot{\theta}$ is proportional to M^n with $n=14$. Therefore, this term is about 2.4% of the value of shear stress. In case of very slow strain rate such as in creep, $n=3\sim5$ and this term may become nearly 10% of the values of τ_a. It can be safely said that for the hot torsion test of aluminum alloys in this work, the second and third term in Equation (3) contribute less than 3 percent of τ_a values whereas the correction by temperature rise increases as increasing strain up to 20 percent.

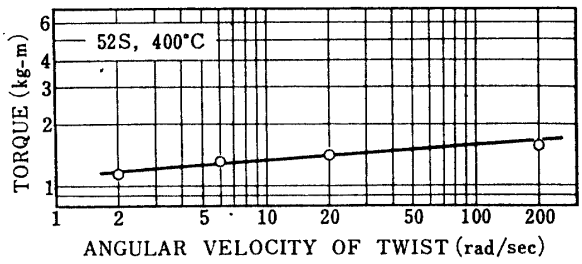

FIG. 4. Logarithmic plot of torque against angular velocity of twist, 52 at 400°C.

Experimentally, three different methods of the torsion test are available. They are; (1) thin walled tubular specimen test, (2) differential test and (3) solid specimen test. In torsional deformation of the thin walled tubular specimens, uniform deformation is assumed and the average shear stress over the cross section is obtained from the measured torque by using the following relation,

$$\bar{\tau}=\frac{3M}{2\pi(a_2^3-a_1^3)} \qquad (5)$$

where a_1 is the inner radius and a_2 is the outer radius. For the tubular specimens, buckling occurs at the early stage of torsional deformation, and changes in the specimen dimensions result. Therefore, Equation (5) can be applied only before buckling starts. For the hot torsion test where deformation is carried out up to high strains, flow stress at higher strain as well as fracture strain of the material can not be evaluated by testing of the thin walled tube specimens.

The differential test, termed by Field and Backofen [5], can provide the average shear stress in a tubular section of the specimen by calculation from the torque difference between two solid specimens of slightly different diameters, a_1 and a_2, by using the following equation,

$$\bar{\tau}=\frac{3}{2\pi}\frac{M_2-M_1}{a_2^3-a_1^3} \qquad (6)$$

The solid specimen test can provide shear stress only at the surface of the specimen as previously mensioned and the values of shear stress obtained are reported to be more self-consistent than by the differential method [6].

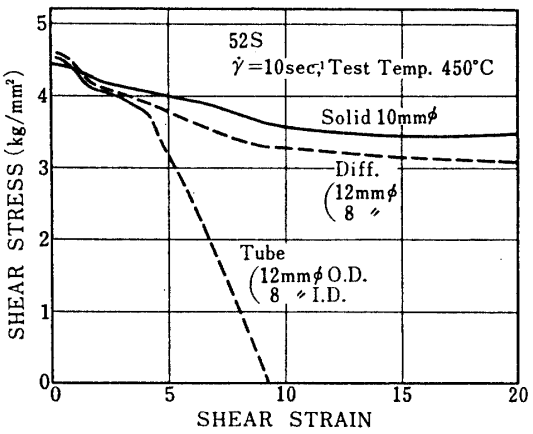

FIG. 5. The shear stress-strain curves obtained by the thin-walled tubular specimen test, the differential test and the solid specimen test.

One example of comparison of these three methods is shown in Fig. 5 for 5052 alloy specimens tested at 450°C at strain rate 10 sec^{-1}. This shows that the maximum shear stresses are all within the experimental error, whereas flow stress values at higher strain are quite different each other. Flow stress decreases rapidly. in the tubular specimen test due to buckling of the specimen. For the differential method, flow stress values are lower than by the solid specimen test at higher strain and this is explained by the effect of temperature rise. For the specimen of slightly smaller diameter, there is no heat flow coming in from outside during deformatian, whereas to the equivalent portion of the specimen of the larger diameter heat flow comes in from the outernal layer. In the differential test, not only reproducibility of shear stress values has been reported to be poor, [6], but also determination of fracture strain is somewhat uncertain. The solid specimen test is simple and easy to carry out. Therefore, it is concluded that the solid specimen test is most suitable for evaluating hot workability of aluminum alloys.

4. Temperature Rise During Torsional Deformation

It is important to discuss the effect of temperature rise in the specimen during deformation on the test results, since deformation is carried out at high strain rate

up to very high stain, that is, considerable amount of work which causes heat generation is done to the specimen. Thus, the temperature change of the specimen was measured during torsional deformation.

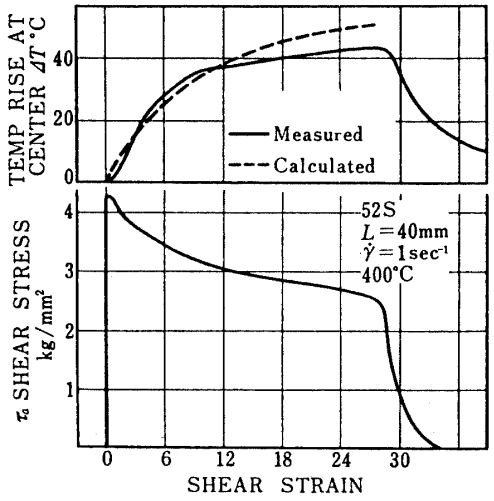

FIG. 6: The measured temperature change during torsional deformation and the corresponding shear stress-strain curve.

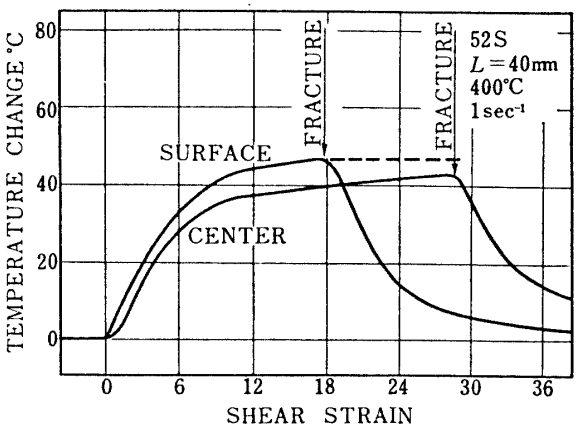

FIG. 7: The measured temperature change during torsional deformation at the middle-center and the middle surface of the specimen.

Eig. 6 shows an example of the measured temperature changes at the middle-center of the specimen during torsional deformation. Here, the corresponding shear stress-shear strain curve is also shown, and it is seen that temperature continues to rise until fracture occurs. The maximum temperature corresponds to the temperature when fracture occurs. In Fig. 7, temperature rise at the middle-surface is compared with that at the middle-center of the specimen. Insertion of a thermocouple at the surface caused the notching effect, and fracture occurred at lower strain whereas very little change was caused by insertion of a thermocouple at the middle-center through the thin hole drilled along the center axis of the specimen where very little torsional deformation is done. Therefore, the comparison could not be done for the same range of strain. However, heat flux to the center decreases the difference in temperature

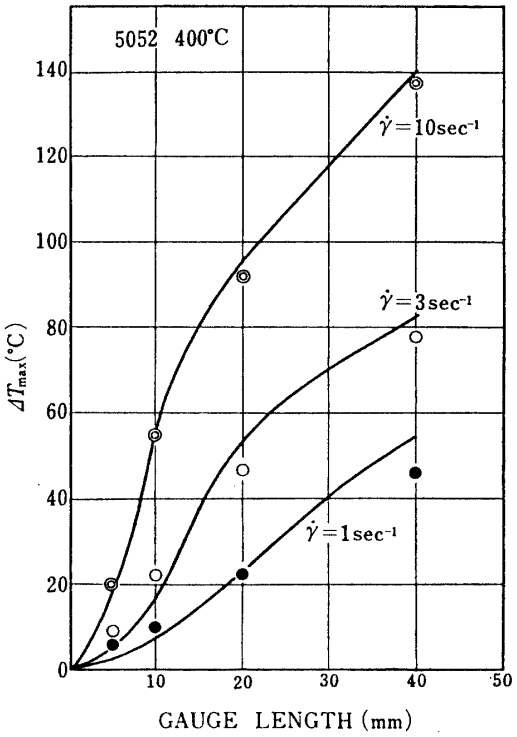

FIG. 8. The maximum temperature rise plotted against the specimen guage length for different strain rate, curves represent the calculated values.

rise between center and surface of the specimen as increasing strain as shown in the extended dotted line.

In Fig. 8, each point represents the observed maximum temperature rise at the middle-center of the specimen of the different gauge length tested at different strain rates. The curves in this figure represent the calculated values, which reasonably agree with the corresponding observed ones. Calculation is done by using the following equation, of which derivaration is presented in Appendix,

$$\Delta T=\frac{Al^2}{K}\left\{\frac{3}{2}-\frac{64}{\pi^3}\sum_0^{\infty}\frac{(-1)^n}{(2n+1)^3}\cos\frac{(2n+1)\pi}{4}\exp\left[-\kappa(2n+1)^2\pi^2t/16l^2\right]\right\} \quad (7)$$

where A: average heat generation by deformation (cal cm^{-3} sec^{-1})
l: half of guage length (cm)
K: heat conductivity of the specimen (cal/cm sec °C)
κ: heat diffusivity of the specimen (cm^2 sec^{-1})
t: time from the start of deformation (sec).

The dotted line in Fig. 6 also represents the calculated values by Equation (7). The calculated values are slightly higher than observed ones at higher strain because of decrease in flow stress as increasing strain, although a reasonable agreement is obtained as a whole. By using Equation (7), $\Delta T/A$ is plotted against t for the specimens of different guage length in Fig. 9. When the average flow stress and strain rate are known, the value A is determined and temperature rise can be estimated from this figure. It is shown that for shorter specimens temperature rise

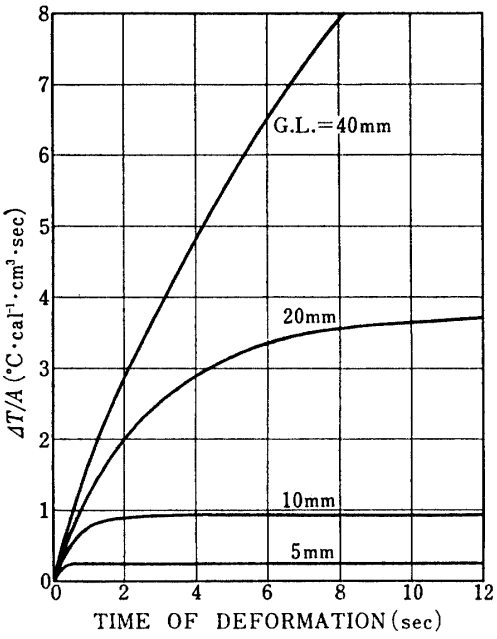

FIG. 9. The calculated value of temperature rise at the middle of the specimen time of deformation for different guage length.

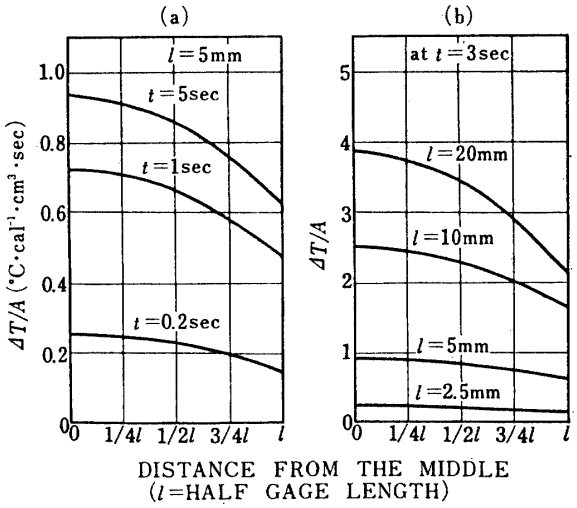

FIG. 10. The distribution of temperature rise, (a) for different time of diformation and (b) for different guage length.

reaches a plateau in shorter time.

Distribution of temperature rise along the longitudinal axis of the specimen can be expressed by Equation (J) given in Appendix. Calculated values for different amount of strain and for different guage length are plotted in Fig. 10. It is seen from these curves that nonuniformity in temperature in the specimen during torsional deformation increases as increasing either strain or guage length.

Temperature rise during deformation, which has been discussed above, causes changes in flow stress. Now, a method of estimation of temperature rise has been presented, decrease in flow stress can also be estimated and flow stress values at a constant temperature are obtainable by using Equation (4).

5. Strain Distribution

Nonuniform distribution of temperature rise in the axial direction of the specimen during torsional deformation causes nonuniform flow stress, and hence, nonuniform distribution of strain in this direction. Strain distribution was measured in the following way. A straight line marking was initially drawn parallel to the specimen axis. This specimen was taken out of the testing machine after a certain num-

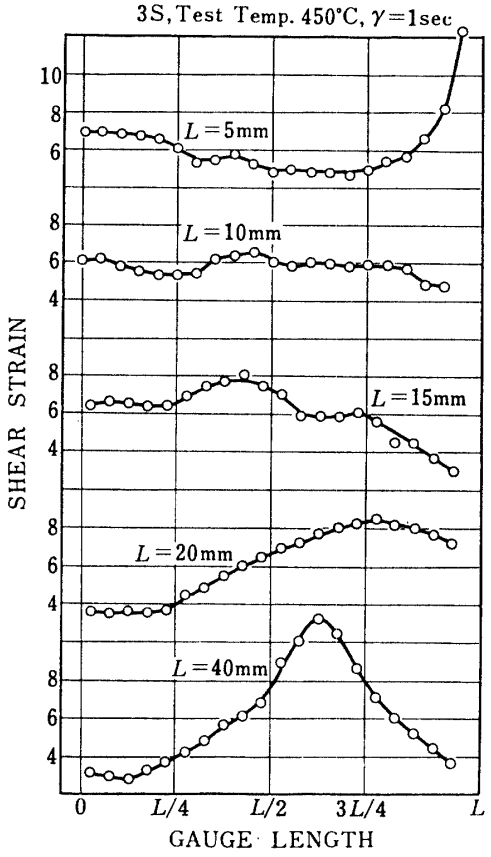

Fig. 11. The distribution of shear strain at the surface along the axial direction for different specimen guage length.

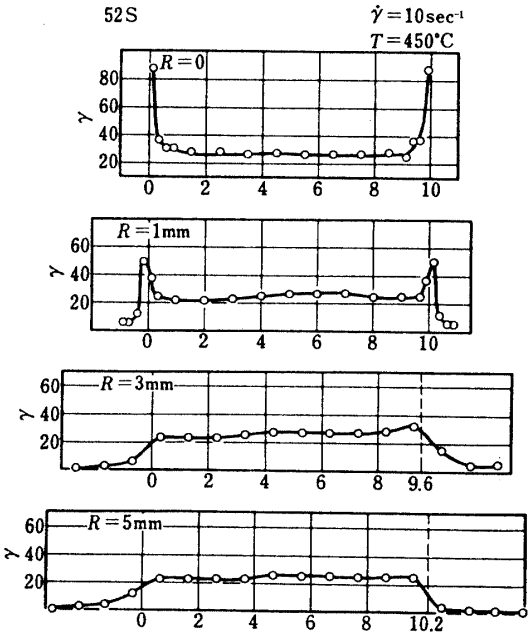

Fig. 12. The strain distribution of the surface of specimens of various fillet radii of the alloy 5052.

ber of twists before fracture occurs. Local strain on the surface was determined in the longitudinal direction by examining the marking which was deformed to be a helical line after torsional deformation.

In Fig. 11, strain distribution is shown for 3003 alloy specimens deformed at 450°C at strain rate 1 sec^{-1} for the specimens of different guage length. Strain tends to concentrate near the middle of the guage section for the specimens longer than 15 mm, whereas strain concentration occurs at both ends of the gage part for the specimen 5 mm long. The stress concentration factor at the fillet for the specimen shown in Fig. 2 with $r=0.5$ mm is 1.8 [7]. It is now evident that strain concentration near the middle is caused by temperature rise during torsional deformation, and that at both ends due to the change in cross sectional area at the fillet when temperature rise is not significant as shown in Fig. 9. Since stress concentration factor decreases with increasing fillet radius r, strain concentration at the fillet decreases with increasing r as shown in Fig. 12 for the 52S alloy specimens with $L=10$ mm. However, length of the deformed part of the specimen exceeds the geometrical gage length as increasing fillet radius, and the effective gage length

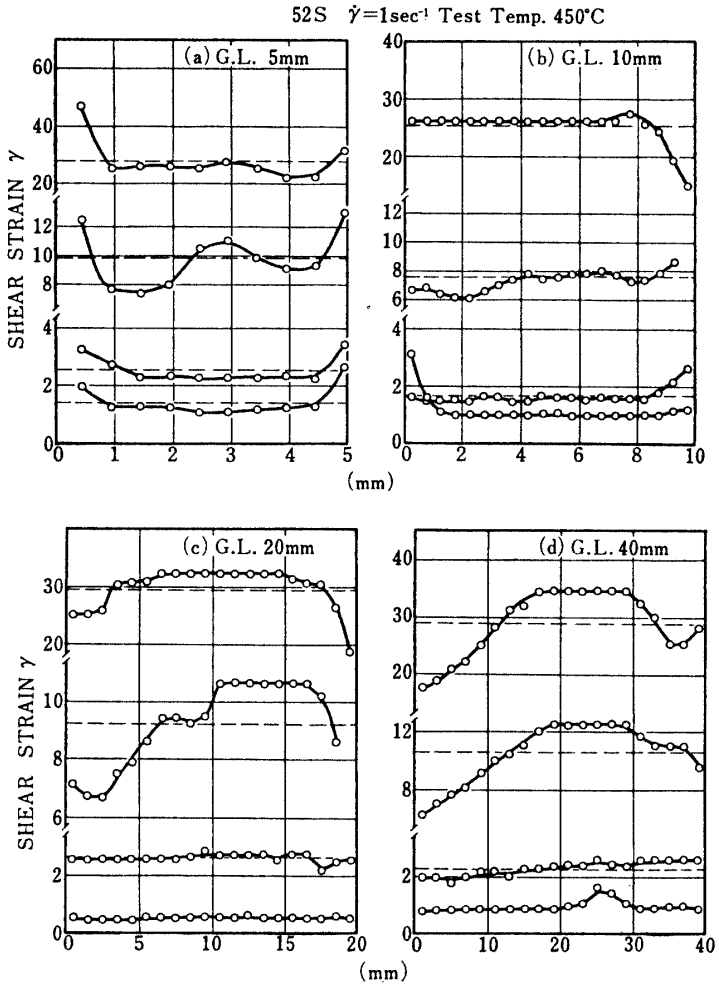

Fig. 13. Shear strain clistribution at various stages of deformation.
(a) $L=5$ mm (b) $L=10$ mm (c) $L=20$ mm (d) $L=40$ mm

becomes difficult to be specified depending on the testing conditions. Therefore, smaller r is desirable for the consistency of effective gage length, and larger r is preferred for more uniform strain distribution. Thus, some compromise is necessary to determine fillet radius, and $r=0.5$ mm was taken in this work. The non-uniformity in strain distribution was observed to increase as deformation proceeds, and finally fracture occurs at the point of maximum strain. The change in strain distribution at different stages of torsional deformation is shown in Fig. 13 for the specimens of different gage length, 5, 10, 20 and 40 mm.

In Fig. 14, shear stress-shear strain curves are shown for 5052 alloy specimens of different guage length twisted at 450°C. It is seen that the longer specimen has lower value of flow stress in the high strain region. From the foregoing results, it is clear that the more uniform strain distribution can be attained if the specimen has shorter guage length and larger fillet radius. However, larger fillet radius with shorter guage length makes the effective length of the guage section, where torsional deformation takes place, uncertain, as stated above. From the experimental results above, the most suitable specimen dimensions, from the standpoint of uniform strain distribution in the longitudinal direction, are 10 mm in diameter and guage length for $r=0.5$ mm, for the present study of hot workability of aluminum alloys.

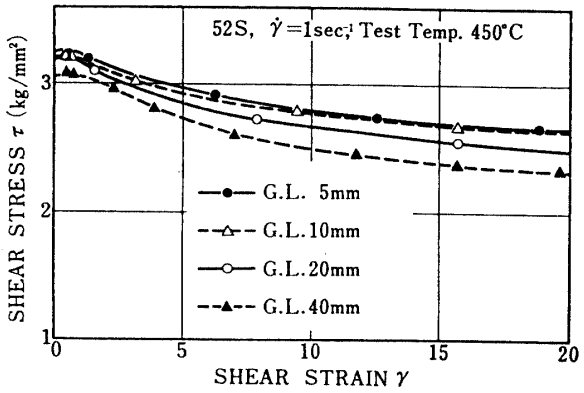

FIG. 14. The shear stress-strain curves for different specimen guage legth.

6. AXIAL STRAIN DURING TORSIONAL DEFORMATION

It has been known for long that the change in length in the longitudinal direction of the specimen occurs during torsional deformation of metals [*8*]. Hill [*9*] has explained that this axial strain is caused by plastic anisotropy. However, it has the marked temperature dependency, and the whole mechanism seems to have not been made clear. It has been reported that elongation occurs at lower temperature and the axial elongation decreases with rising testing temperature and it starts to shrink as torsional deformation proceeds at above a certain temperature. Axial shrinkage has been reported to be related to recrystallization occurring during deformation for steels [*10*]. Lead is reported to show axial shrinkage even at room temperature.

The amount of axial strain at the fracture point is shown in Fig. 15 for 5056 alloy specimens at different testing temperature and strain rates. It is seen that the transition from elongation to shrinkage occurs at higher temperature as increasing strain rate. Temperature dependency of the amount of axial strain is more

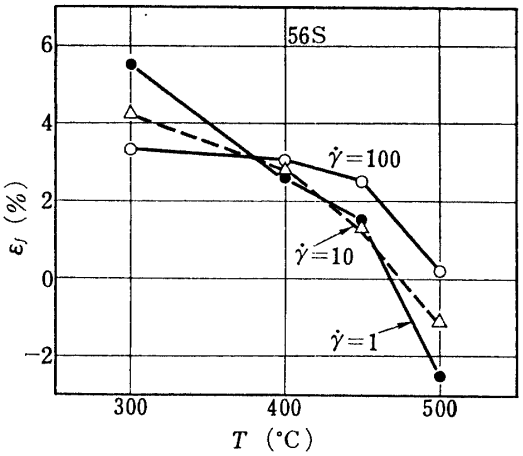

FIG. 15. Axial strain due to torsional deformation at the fracture point plotted against testing temperature for different strain rate.

pronounced for lower strain rate, probably because fracture strain has higher temperature dependency for lower strain rate. For this alloy in this temperature range, the amount of axial elongation after one twisting revolution is found to be larger for higher strain rate. Fig. 15 shows the results obtained for the specimens machined from the extruded bars, but the values obtained from the direct-chill cast ingots of the same alloy showed the almost identical results.

7. STRAIN TO FRACTURE

Fracture strain is generally considered to represent ductility of the material tested. Although both flow stress and ductility are considered here to determine hot workability, ductility is much more important factor of hot workability particularly for the relatively poorly ductile aluminum alloys such as duralmin and Al-Mg alloys. However, evaluation of fracture strain is not so simple because it varies sensitively with the specimen shape and dimensions as show in Figs. 16 and 17. In Fig. 16, variation of fracture strain for the specimens of 10 mm diameter with different guage length are shown for 5056 and 2017 alloys. Fracture strain decreases with

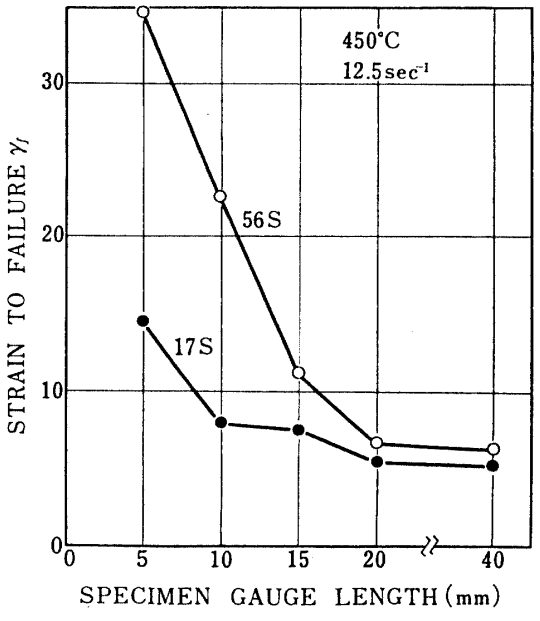

FIG. 16. Fracture strain plotted against specimen guage length for the specimens of the alloys 2017 and 5056

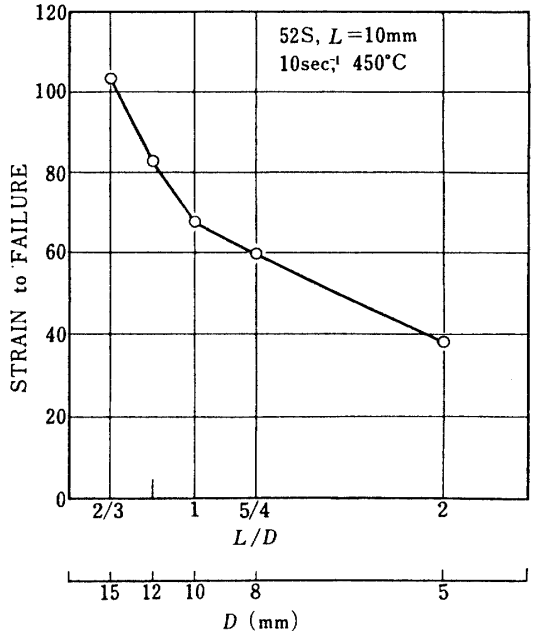

FIG. 17. Fracture strain plotted against the specimen diameter.

increasing specimen guage length, and this result is easily understood by the foregoing results of temperature rise and strain distribution. It is now seen that the comparison of fracture strain for the specimens of different guage length is meaningless in evaluating ductility of the materials.

In Fig. 17, fracture strain for the specimens of 10 mm guage length are plotted against diameter of the guage part. As decreasing diameter, fracture strain decreases because nonuniformity in temperature distribution in the specimen is more pronounced for the specimen of smaller diameter. In Fig. 18, the values of fracture strain are plotted against tensile stress in the axial direction. This was obtained from the tests when the axial tensile load is applied during torsional deformation. It is shown that fracture strain decreases drastically with tensile stress, and that the effect of temperature on the values of fracture strain is reversed when the tensile stress is more than about 0.1 kg/mm². For very ductile alloys such as 1100 or 3003 which often show no distinct fracture point on the stress-strain curves when deformed at high temperature, a distinct fracture point may appear when twisted under the presence of the tensile stress in the axial direction. However, it should be noted that the values thus obtained are different in character from those obtained by pure torsional deformation.

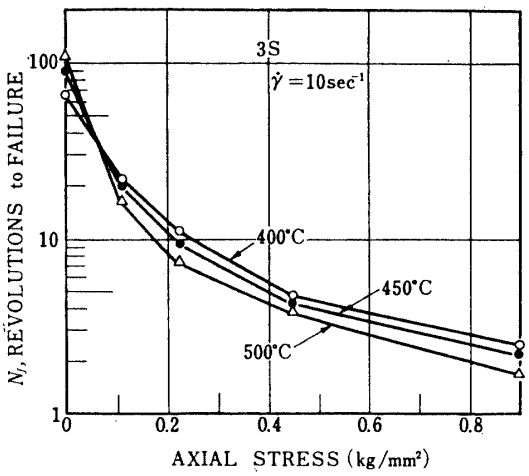

FIG. 18. Fracture strain plotted against tensile stress applied during torsional deformation for different testing temperature.

When torsional deformation is carried out with the both ends constrained for axial strain, axial internal stress will result corresponding to axial strain which appear with an unconstrained end, as previously stated. Since this internal axial stress varies with testing temperature, torsional strain and strain rate, the values of fracture strain obtained with the constrained end test are, therefore, not suitable for discussing the effects of testing temperature and strain rate on ductility.

Tubular specimens are not suitable for evaluating fracture strain because buckling occurs during torsional deformation and the values of fracture strain are poorly reproducible in the hot torsion test. As mentioned above, fracture occurred at considerably lower strain for the specimen of which temperature rise was measured at the middle-surface. This means that any surface defects may affect the values of fracture strain and that the specimen has to be machined with a great care.

Thus, the values obtained for fracture strain in the hot torsion test, which are liable to be affected by various testing conditions, may have little meaning in an absolute scale. However, if careful evaluation is done, fracture strain in the hot torsion test can be a reliable measure for ductility of metals under hot working conditions obtained in the laboratory test.

8. Summary

Hot workability depends both on the material properties and on the deformation conditions. The hot workability test is done by simulating the actual hot working processes by simplifying the stress-strain conditions. Therefore, there always exist certain limitations for applying the test results to the actual hot working processes, besides they do not represent the true properties of the material tested. In the hot torsion test, deformation can be carried out at a constant strain rate up to very high strain for a wide range of strain rate. It is a suitable laboratory testing method for the evaluation of hot workability of metals since deformation can cover the range of most industrial hot working processes. The most suitable testing conditions have been discussed for evaluating hot workability of aluminum alloys by means of the hot torsion test. Also, a detailed discussion has been given for the characteristics of this testing method. The obtained results are summarised as follows:

(1) The solid specimen test is the most suitable method for evaluation of both flow stress and ductility among three methods of torsion tests; the thin-walled tubular specimen test, the differential test and the solid specimen test.

(2) Considerable temperature rise occurs in the deformed part of the specimen when deformed at high strain rate and up to high strain. The amount of temperature rise was found to increase with the specimen guage length or with strain rate. A method of estimation of temperature rise is presented, with which experimentally measured values reasonably agree. The shear stress-shear strain curves at a constant temperature, i.e. stress corrected for temperature rise, are obtained by estimating temperature rise, and remain to show a distinct effect of strain rate in the high strain region. Decrease in flow stress due to temperature rise is shown to be as large as 20 per cent in the torsion test of aluminum alloys.

(3) Nonuniform torsional strain distribution in the axial direction results from nonuniform temperature rise due to heat conduction. Nonuniformity in strain distribution which varies fracture strain sensitively, is affected by the specimen shape and dimensions. It is therefore necessary to determine the specimen shape and dimensions so as to keep distribution of both temperature rise and shear strain in the axial direction as uniform as possible. From the experimental results obtained, the most suitable specimen shape and dimensions for the study of hot workability of aluminum alloys which is now being carried out at this laboratory, are determined to be a solid cylinder with 10 mm guage length and 10 mm diameter and with 0.5 mm fillet radius.

(4) It is desirable to keep the specimen end unconstrained for axial strain during torsional deformation. For proper evaluation of fracture strain, torsional deformation with both ends of the specimen constrained or under the presence of tensile stress in the axial direction is not recommended.

(5) The maximum shear stress can serve as a measure for deformation resistance. Since it appears at shear strain less than unity, little temperature rise occurs at this stage of deformation and no correction for temperature rise and strain

hardening is necessary. The correction term for strain rate dependency is less than 3% of shear stress under hot working conditions.

APPENDIX Estimation of Temperature Rise

The actual situation of temperature rise in the solid cylindrical specimen during torsional deformation is very complicated. In order to consider this problem analytically, a simplified one-dimensional model is considered, and estimation of temperature rise is done by using the obtained solution. A reasonably good agreement is attained with the measured values. Drivaration of this solution is presented below.

The assumptions considered here are as follows;

(a) Heat generation is uniform over the deformed section of the specimen and does not vary with strain. Amount of heat generation, A (cal/cm^{3}sec), is given in terms of average stress and strain as,

$$A=\frac{1}{J\cdot t_f}\int_0^{\bar{\gamma}_f}\bar{\tau}d\bar{\gamma}=\frac{2}{3}\frac{\dot{\gamma}_a\bar{\tau}}{J} \tag{A}$$

where t_f: time to fracture (sec)

J: mechanical equivalent of heat

$\dot{\gamma}_a$: shear strain rate at the surface (sec^{-1})

$\bar{\tau}$: average shear stress, and $\bar{\gamma}$: average shear strain over the cross section.

(b) Heat transfer away from the specimen surface is negligibly small, this will be discussed later.

(c) A constant cross sectional area for heat conduction in the specimen.

Taking x in the axial direction with $x=0$ at the middle of the guage section, and guage length being $2l$, the following differential equations for nonsteady heat conduction hold during torsional deformation,

$$\frac{\partial^2\Delta T}{\partial x^2}-\frac{1}{\kappa}\frac{\partial\Delta T}{\partial t}+\frac{A}{K}=0, \qquad 0<x<l \tag{B}$$

$$\frac{\partial^2\Delta T}{\partial x^2}-\frac{1}{\kappa}\frac{\partial\Delta T}{\partial t}=0, \qquad l<x \tag{C}$$

with the initial and boundary conditions;

(i) $\partial\Delta T/\partial x=0$, at $x=0$

(ii) $\Delta T=0$, at $x\geqq L(L\geqq l)$

(iii) solution for equations (B) and (C) are continuous at $x=l$

(iv) $\Delta T=0$, when $t=0$.

Laplace transformation yields the following differential equations [*11*],

$$\frac{\partial^2 u}{\partial x^2}-q^2u+\frac{A\kappa}{Kp}=0, \qquad 0<x<l \tag{B'}$$

$$\frac{\partial^2 u}{\partial x^2}-q^2u=0, \qquad l<x \tag{C'}$$

where $q^2=p/\kappa$. The solutions for Equations (B') and (C') are as follows,

$$u=c_1e^{qx}+c_2e^{-qx}+\frac{A\kappa}{Kp^2}, \qquad 0<x<l \tag{D}$$

$$u=c_3e^{qx}+c_4e^{-qx}, \qquad l<x \tag{E}$$

The constants c_1, c_2, c_3 and c_4 are determined from the initial and boundary conditions, then Equation (D) becomes,

$$u=\frac{\kappa A}{Kp^2}\left[1-\frac{e^{ql}+e^{2qL}e^{-ql}}{2(1+e^{2qL})}(e^{qx}+e^{-qx})\right], \qquad 0<x<l \tag{F}$$

Now, three cases for the values of L are considered, they are,

(I) $L=\infty$

(II) $L=l$

(III) $L=2l$.

For the above three cases, solutions for $\Delta T'$ at $x=0$, which are obtained by applying the Laplace Inversion Theorem to Equation (F), are as follows,

(I) $$\Delta T_{x=0}=\frac{\kappa At}{K}\left[1-4i^2\ \mathrm{erfc}\ \frac{l}{2\sqrt{\kappa t}}\right] \tag{G}$$

(II) $$\Delta T_{x=0}=\frac{Al^2}{K}\left[\frac{1}{2}-\frac{16}{\pi^3}\sum_{n=0}^{\infty}\frac{(-1)^n}{(2n+1)^3}\exp\{-\kappa(2n+1)^2\pi^2t/4l^2\}\right] \tag{H}$$

(III) $$\Delta T_{x=0}=\frac{Al^2}{K}\left[\frac{3}{2}-\frac{64}{\pi^3}\sum_{n=0}^{\infty}\frac{(-1)^n}{(2n+1)^3}\cos\frac{(2n+1)\pi}{4}\exp\{-\kappa(2n+1)^2\pi^2t/16l^2\}\right] \tag{I}$$

For the 5052 alloy specimens of different guage length, deformed at 400°C at strain rate 3 sec^{-1}, temperature rise was measured. In Fig. 19, the points represent observed temperature rise at the maximum values, and the cureves the calculated values by using above three equations, (G), (H) and (I). It is shown that the calculated values by Equation (I) agree best with the observed ones among three cases considered. Equation (G) overestimates the actual temperature rise, whereas Equation (H) underestimates, which is quite reasonable judging from the boundary condition considered for each case.

In Fig. 5 previously shown, the calculated values of the maximum temperature rise by Equation (I) are plotted and compared with the observed ones for different strain rate and guage length. Agreement is reasonably good in general, although

there exists some systematic deviation from the observed values, the estimated values by Equation (I) are slightly lower for shorter guage length and slightly higher for longer guage length.

The numerical values of temperature rise, $\Delta T_{x=0}$, calculated by using Equation (I), are plotted against surface shear strain for different strain rates in Fig. 20. It is shown that the higher strain rate or the longer specimen gauge length, the more temperature rise becomes adiabatic. Therefore, the values of $\Delta T_{x=0}$ are markedly affected by the specimen gauge length at lower strain rate. In Fig. 20, the values of $\Delta T_{x=0}$ are calculated for $\bar{\tau}=4\ \mathrm{kg/mm^2}$. Since $\Delta T_{x=0}$ is proportional to $\bar{\tau}$ as readily seen in Equations (A) and (I), the values of $\Delta T_{x=0}$ for any $\bar{\tau}$ values are easily obtained by simply multiplying $\bar{\tau}/4$. For this purpose, the typical values of $\bar{\tau}$ for the ingots of various wrought aluminum alloys, which have been obtained in this laboratory, are listed in Table 2 for different strain rate and testing temperature. By using this table and Figure 20, the values of $\Delta T_{x=0}$ are easily estimated for various testing conditions. Note that this estimation procedure for $\Delta T_{x=0}$ is restricted to aluminum alloys since the unique values of κ and K are substituted for obtaining the values shown in Figure 20.

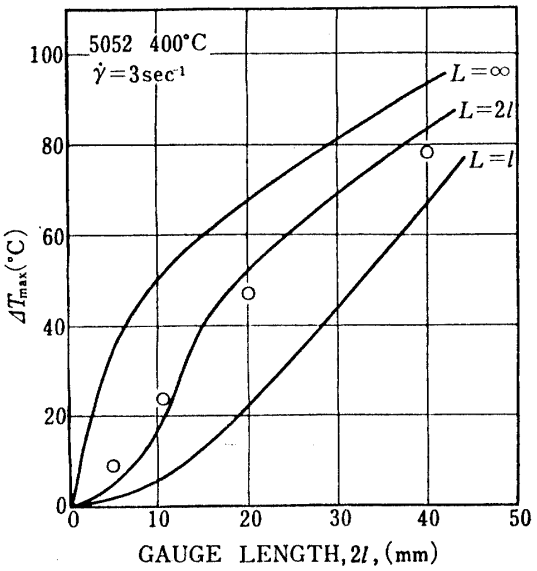

FIG. 19. The calculated values of the maximum temperature rise obtained from the different boundary conditions and compared with the measured values.

It is now seen that temperature rise during torsional deformation can be properly estimated with the boundary condition, $L=2l$, distribution of temperature rise in the guage section, that is, for $0<x<l$, can be expressed in the following equation, which is obtained by solving Equation (F) in the same way as for Equations (G), (H) and (I).

$$\Delta T=\frac{Al^2}{K}\left[\frac{3}{2}-\frac{x^2}{2l^2}-\frac{64}{\pi^3}\sum_{n=0}^{\infty}\frac{(-1)\pi}{(2n+1)^3}\cos\frac{(2n+1)\pi}{4}\cos\frac{(2n+1)x\pi}{4l}\right.$$
$$\left.\exp\{-\kappa(2n+1)^2\pi^2t/16l^2\}\right] \qquad \text{(J)}$$

Heat transfer away from the specimen surface is considered below. The amount of heat loss from the surface, Q (cal/cm²sec), is expressed as $Q=h\cdot\Delta T$, where h is heat transfer coefficient of the specimen surface, cal/sec °C cm². Now, we need to evaluate the value of h in our experimental conditions. Since heat transfer from the surface is considered to take place in forced convection with the laminar boundary layer, h is generally expressed as follows [*12*],

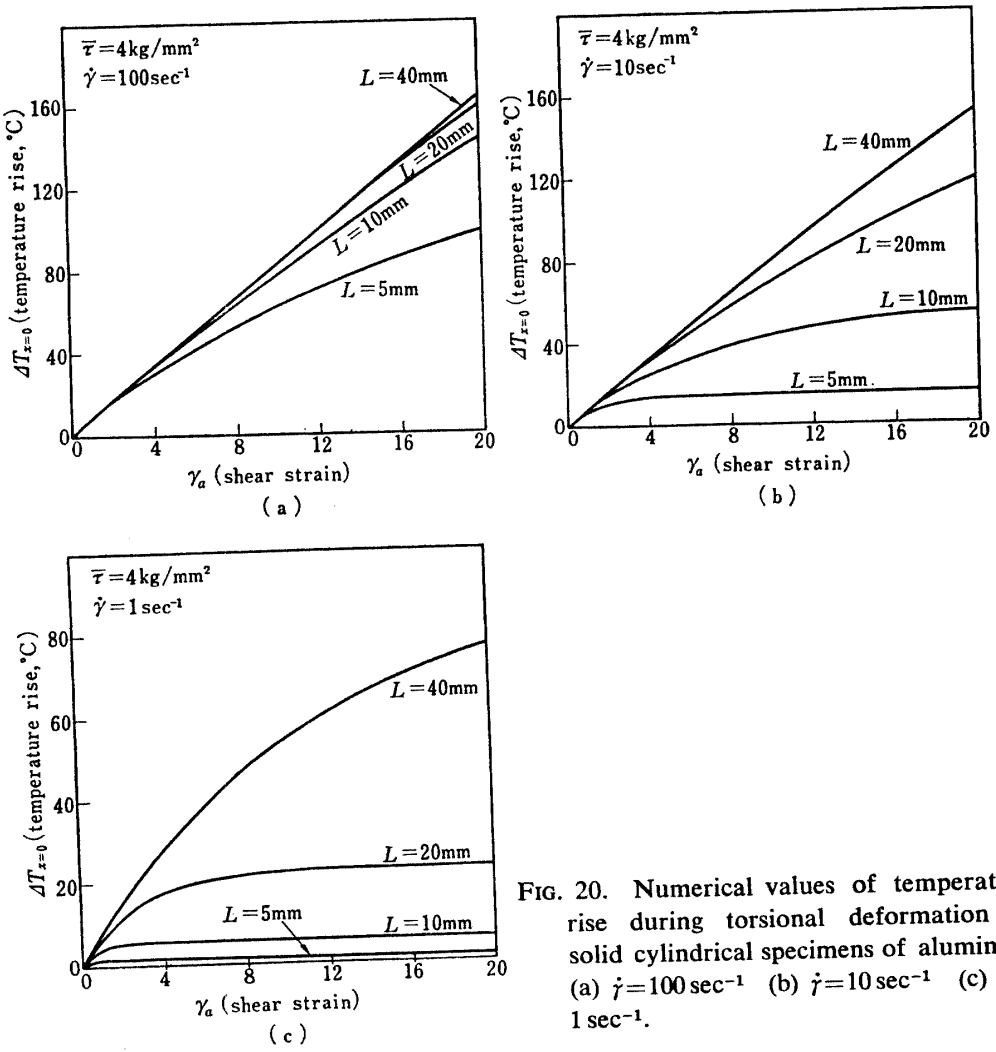

FIG. 20. Numerical values of temperature rise during torsional deformation of solid cylindrical specimens of aluminum (a) $\dot{\gamma}=100\,\text{sec}^{-1}$ (b) $\dot{\gamma}=10\,\text{sec}^{-1}$ (c) $\dot{\gamma}=1\,\text{sec}^{-1}$.

TABLF 2. Typical values of $\bar{\tau}$(kg/mm²) for the ingots of the various wrought aluminum alloys

$\dot{\gamma}$	1 sec⁻¹			10 sec⁻¹			100 sec⁻¹		
°C	400	450	500	400	450	500	400	450	500
1100 (2S)	1.5	1	1	2	1.5	1.5	2.5	2	1.5
3003 (3S)	2	1.5	1	2.5	2	1.5	3	2.5	2
2014 (14S)	3	2.5	2	4	3.5	3	5	4	3.5
2017 (17S)	4	3	2	5	4.5	4	6	5	4.5
5052 (52S)	3.5	3	2	4.5	3.5	2.5	5.5	4.5	3.5
5056 (56S)	5	3.5	3	7	5.5	4.5	9	7.5	6
5083 (NP5/6)	5.5	4	3	7	5.5	4.5	8	7.5	6
6063 (63S)	2	1.5	1	2.5	2	1.5	3	2.5	2
Al-Zn-Mg (74S)	3	2	1.5	4	2.5	1.5	4.5	4	3
7075(75S)	4	3	—	5	4	—	—	—	—

$$h=0.332\,\kappa\,\sqrt[3]{P_r}\sqrt{\frac{v_s}{\nu x}} \qquad \text{(K)}$$

where P_r: Prandtle number of air
v_s: surface velocity of twisting (cm/sec)
ν: kinematic viscosity of air.

Taking $x=\pi r/4$ in our case, the value of h for air at 400°C for 10 mm diameter specimens at the angular velocity of twist, $\dot{\theta}$, is expressed as $h\cong 1.6\times 10^{-7}\sqrt{\dot{\theta}}$. Therefore, h is of the order of 10^{-6} cal/sec °C cm^2.

When heat generation due to work of deformation is converted to per specimen surface area in the deformed section of 10 mm diameter, A' (cal/sec cm^2), it becomes that $A'=A/4$. Thus, the value of A' for 5052 alloy is of the order of surface shear strain rate, that is, 1 to 100 cal/sec cm^2. Within the range of the experiments in this work, heat transfer away from the specimen surface is completely negligible. Thus, Assumption (b) is satisfied. If heat transfer from the specimen surface is not negligible, heat loss is maximum at the twisting end of the guage section and nearly zero at the fixed end, as is clearly seen from Equation (K). In this case, the peak in temperature distribution may shift towards the fixed end from the middle of the guage section.

Department of Materials
Institute of Space and Aeronautical Science
University of Tokyo, Tokyo
January 10, 1970

References

[1] W. J. McG. Tegart: *Ductility*, Amer. Soc. Metals, (1968), 133.
[2] F. A. Hodierne: J. Inst. Metals, **91**, (1962/63), 267.
[3] J. L. Robbins, H. Wagnaar, O. C. Shepard and O. D. Sherby: J. Materials, **2** (1967), 267.
[4] M. Tsubouchi and H. Kudo: Sosei to Kako, **9** (1968), 332.
[5] D. S. Fields, Jr. and W. A. Backofen: Proc. Amer. Soc. Materials, **57** (1957), 1259.
[6] D. S. Fields, Jr. and W. A. Backofen: Trans. ASM, **51** (1959), 946.
[7] S. Timoshenko, J. N. Goodier: Theory of elasticity, 2nd ed., McGraw-Hill, (1950).
[8] H. W. Swift: Engineering, **4** (1947), 253.
[9] R. Hill: *Mathematical Theory of Plasticity*, Oxford, (1950).
[10] F. Morozumi: Tetsu to Hagane, **52** (1966), 1859.
[11] H. S. Carslaw and J. C. Jaeger: *Conduction of Heat in solids*, Oxford, (1959), 297.
[12] E. R. G. Eckert and R. M. Drake, Jr.: *Heat and Mass Transfer*, (2nd Ed.) McGraw-Hill, New york, (1959), 167.